The OCS S L_3MM Auger Spectrum and Angular Distributions Studied by Photoelectron−Auger Electron Coincidence Experiments†

P. Bolognesi,‡ P. O'Keeffe,‡ and L. Avaldi*,‡,§

CNR-IMIP, Area della Ricerca di Roma, CP10, 00016 Monterotondo Scalo, Italy, and CNR-INFM-TASC, Gas Phase Beamline at Elettra, Area Science Park, Basovizza (Trieste), Italy

Received: June 5, 2009; Revised Manuscript Received: July 19, 2009

The selectivity of the photoelectron−Auger electron coincidence technique has been used to isolate the S L_3MM contribution to the $L_{2,3}MM$ Auger spectrum in OCS. In this way, a direct comparison of the energies, widths, and relative intensities of the final OCS^{2+} states with theoretical calculations has been achieved. Moreover, the angular distributions of some selected Auger electrons have been measured in coincidence with the photoelectron at two different photon energies. In contrast with the results of noncoincidence measurements, the coincidence angular distributions show a significant asymmetry and a dependence on the photon energy and OCS^{2+} final state.

1. Introduction

Auger electron spectroscopy has become one of the most used analytical techniques[1] to characterize the composition of materials and to study the effects of the chemical environment on the emitter atom. Despite the widespread applications of the technique, the interpretation of molecular Auger spectra and the understanding of the dynamics of the process and of the angular distribution of the Auger electrons are still attracting much interest. The interpretation of the molecular Auger spectra represents a complicated problem because of the large number of states of the doubly charged ion that can be formed. Ionization and decay of an inner shell involve three molecular states, namely, the ground state of the neutral species, the state of the singly charged ion with its inner hole, and the final state of the doubly charged ion. These states differ in their potential energy curves. Therefore, molecular Auger spectra are often characterized by bandlike structures resulting from the interplay of vibrational excitation in the singly and doubly charged ion states. Because of this, the detailed analysis achieved by theoretical models[2] can be compared with experimental results only by summing over all levels of vibrational excitation in the states involved. Moreover, in the case of the spin−orbit splitting of the p, d, or higher l core holes, which gives rise to two levels with different total angular momentum, the Auger decay of these two levels into the same final state manifold produces two sets of electronic transitions separated in energy by the difference between the two levels. Further complexity is added by the presence of two or more atoms of the same element. This is due to the superposition of the decay processes originating from atoms of the same species but located in different molecular sites. These spectra are shifted in energy, and their relative intensity is determined by the different sensitivity of each atom to electronic relaxation and correlation effects.

In 1978, Haak et al.[3] showed that photoelectron and Auger electron spectroscopies can be combined in a technique where these two free but correlated electrons are detected in coincidence. This angle-resolved coincidence experiment results in the measurement of the triply differential cross section $d^3\sigma/d\Omega_1 d\Omega_2 dE_1$ (TDCS), where Ω_1 and Ω_2 are the angles of emission of the two electrons and E_1 is the energy of one of them. The energy of the other electron is defined by energy conservation $h\nu = I^{2+} - E_1 + E_2$, where $h\nu$ is the photon energy and I^{2+} is the double ionization potential of the particular final state of interest. The coincidence technique adds "state and site" selectivity to the conventional Auger measurements, producing a better and unambiguous spectroscopic characterization of the decay electron spectra[4,3] and a deep insight into the two constituent processes.[5,6] Moreover, with the use of high-energy resolution in both the photoelectron and Auger channels, the coincidence experiment, via the energy conservation, allows the limitation imposed on Auger spectroscopy by the core-hole lifetime to be overcome.[7]

In the molecular case, the photoelectron−Auger electron coincidence technique, via the selection of a photoelectron of well-defined kinetic energy, allows the disentanglement of the contributions from different vibrational levels and spin−orbit components of the core level and of atoms at different sites. To investigate all of these different facets of the Auger decay following molecular inner shell photoionization, we have undertaken a series of photoelectron−Auger electron coincidence experiments at the gas-phase photoemission beamline[8] at Elettra (Trieste). In two recent works, we have used (i) the site selectivity of the technique to separate the contribution of the terminal and central N atoms from the N_2O Auger spectrum[9] and (ii) the vibrational resolution of the XPS spectrum to investigate the partial Auger yield for vibrationally selected CO^+ (C1 s^{-1}) states.[10] Here the same technique is used to isolate the S $2p_{3/2}{}^{-1}$ contribution to the S 2p Auger spectrum in OCS.

In 1980, Dill et al.[11] showed that the Auger decay of K-shell-excited/ionized molecules should have an anisotropic angular distribution because of the alignment of the intermediate state, which depends on its symmetry. Angular anisotropy in the CO[12] and N_2[13] 1s → π^*,σ^* resonant Auger has been observed. Recently, Semenov et al.[14] have performed an extended theoretical study of the angular distribution of molecular Auger electrons, including the angular distributions from fixed-in-space molecules and Auger electron−photoelectron angular correlations.

† Part of the "Vincenzo Aquilanti Festschrift".
* Corresponding author.
‡ CNR-IMIP.
§ CNR-INFM-TASC.

10.1021/jp9053007
Published on Web 08/06/2009

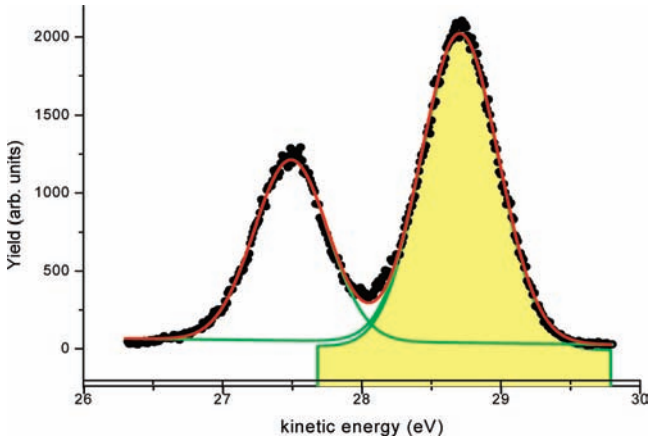

Figure 1. S 2p photoelectron spectrum measured at 200 eV photon energy.

Whereas some information is available in the literature on the angular distribution of S 2p photoelectrons in randomly oriented[15,21] and fixed-in-space[16,17] OCS molecules, to our knowledge, only a value of the asymmetry parameter averaged over the full $L_{23}MM$ auger spectrum has been reported by Truesdale et al.[15] Here the angular distribution of the Auger electrons emitted following the photoionization of the S 2p states has been measured with and without coincidence with the photoelectron.

2. Experimental Section

The experiments have been performed using the multicoincidence end station[18] of the gas-phase photoemission beamline[8] of the Elettra storage ring in Trieste, Italy. The light source is an undulator of period 12.5 cm, 4.5 m long. The linearly polarized radiation from the undulator is deflected to the variable-angle-spherical grating monochromator[19] by a prefocusing mirror. The monochromator consists of two optical elements: a plane mirror and a spherical grating. Five interchangeable gratings cover the energy region from 13 to 1000 eV. Two refocusing mirrors after the exit slit provide a circular spot (radius about 300 μm) at the interaction region in the experimental chamber.

The end station[18] is equipped with 10 independent electrostatic analyzers, arranged in two groups of three, and seven analyzers, respectively, mounted on two separate turntables. For the present experiments, both frames have been kept in the plane perpendicular to the direction of the incoming photon beam, **z**. The analyzer on the small turntable with the field of view placed along the polarization axis of the photon beam has been used to detect the photoelectrons. In the measurement of the coincidence Auger spectrum, photoelectrons of $E_1 = 30$ eV have been selected, whereas in the case of the angular distributions, photoelectrons of 8 and 30 eV, respectively, have been detected to study the ionization and decay of the S 2p state on and off the σ^* resonance.[20] The seven analyzers mounted on the bigger turntable are placed at 30° from each other. They have been used to detect the Auger electrons of energy E_2 between 123 and 143 eV. The energy resolution and the angular acceptance in the dispersion plane of the spectrometers were $\Delta E_i = 180$ and 600 meV for $i = 1$ and 2, respectively, and $\Delta\theta_{1,2} = \pm 4°$. In Figure 1, the S 2p photoelectron spectrum measured at 200 eV and $\theta_1 = 0$ is shown. The energy resolution used in the photoelectron channel enables us to resolve the two S 2p spin−orbit components with their measured splitting of 1.21 ± 0.05 eV, which is consistent with the literature value, but not the molecular-field components of the $2p_{3/2}$ state, whose splitting has been measured to be 145 meV,[21] nor the symmetric stretch vibrational progression (frequency 279 meV[21]). Considering the long lifetime of the S 2p states[21] and the broad energy resolution of the experiment, the effects of postcollision interaction[22] have been neglected in the fit of the photoelectron and Auger spectra. From the fit with a Gaussian function, the relative intensity of the two spin orbit components was found to be 1.8 ± 0.1, as expected because of the slight differences in the asymmetry parameter for the two spin−orbit components determined in the high-resolution measurements by Kukk et al.[21]

The electron signals are processed by a coincidence electronic circuit based on a time-to-digital converter (TDC) unit operated in the common start mode, with the signals of the photoelectron analyzer used as starts and the signals of the Auger electrons used as stops. In this way, seven coincidence pairs are collected simultaneously. All experimental settings and the data acquisition are controlled via a PC equipped with LabView software. The same software monitors the stability of the experiment during the long acquisition times of the coincidence scans via the measurement of the noncoincidence count rates of the eight analyzers and the photon flux at fixed time intervals. In the experiment devoted to the study of the S $2p_{3/2}$ Auger yield of OCS to improve the statistical accuracy of the experimental results, the coincidence signals of the seven photoelectron−Auger electron pairs were added up after a careful energy calibration of the noncoincidence Auger spectra independently collected by the seven analyzers. To calibrate the relative efficiency of the rotatable analyzers in the measurements of the Auger asymmetry parameter β and in photoelectron−Auger electron angular distributions, the well-known angular distribution of Xe $4d_{5/2}$ at about 200 eV incident energy has been measured. From the known β value[23] of this state, the relative angular efficiency corrections have been extracted and applied to both coincidence and noncoincidence raw data. Under the typical experimental conditions of about 8×10^{-6} mbar of gas pressure and 1×10^{11} photon/s, acquisition times of about 1200 and 7200 s/point were needed to achieve the present accuracy in the measurement of the coincidence photoelectron−Auger electron energy and angular distributions, respectively.

3. Results

3.1. S 2p Auger Spectrum. The S $L_{2,3}MM$ Auger electron spectrum and the S L_3MM photoelectron−Auger electron coincidence spectrum, that is, that generated only by the decay of the S $2p_{3/2}$ hole, measured at about 200 eV photon energy are shown in Figure 2. The Figure clearly shows that the peak at the highest kinetic energy in the noncoincidence spectrum corresponds to the decay of the $2p_{1/2}^{-1}$ hole to the ground state of the dication. From the known value of the S $2p_{1/2}$ ionization energy $Ip(2p_{1/2}) = 171.85$ eV[24] and the measured kinetic energies E_A of the S LMM Auger electrons, the double ionization energies, $DIE = Ip - E_A$, of OCS can be obtained. Some measurements of the energy of the OCS^{2+} ground state have been obtained with different techniques, such as electron impact experiments,[25] double charge transfer (DCT) spectroscopy,[26] single-electron capture (SEC) reaction,[27] and "threshold photoelectrons spectroscopy" (TPESCO).[28] High-resolution TPESCO measurements[28] assign the value of 30.0 ± 0.1 eV to the OCS double ionization potential, a value in agreement with those of electron impact experiments[25] and of DCT spectroscopy using OH^+ and F^+ projectiles.[26] The value obtained from our noncoincidence spectrum and confirmed by the coincidence spectrum is 30.35 ± 0.2 eV, which is in agreement with the literature values.

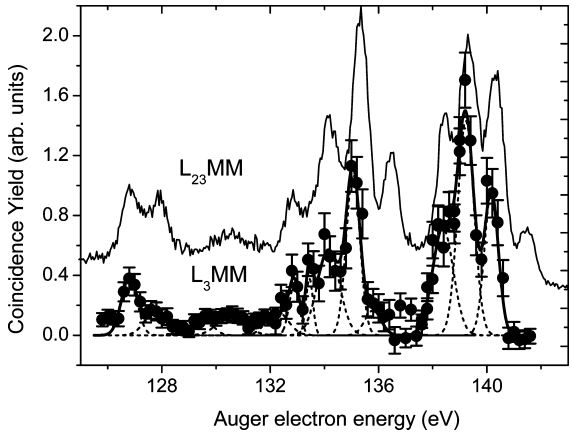

Figure 2. S $L_{2,3}$MM Auger electron spectrum (full line) and the S L_3MM photoelectron−Auger electron coincidence spectrum (dots) measured at 200 eV photon energy.

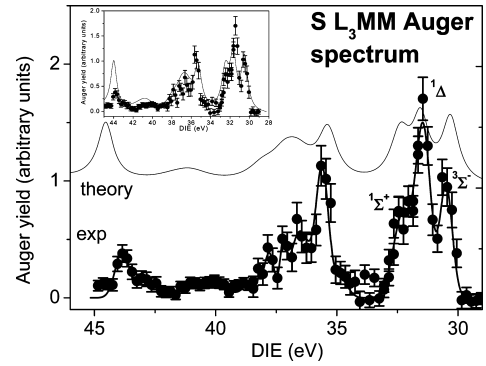

Figure 3. Comparison between the S L_3MM photoelectron−Auger electron coincidence spectrum and the calculations by Minelli et al.[29] In the inset, the energy scale of the theoretical calculation has been contracted by a factor of 0.95.

The electron configuration of OCS ($C_{\infty v}$ symmetry) is (core) $6\sigma^2 7\sigma^2 8\sigma^2 2\pi^4 9\sigma^2 3\pi^4$,[29] where the core includes the S, O, and C 1s and the S 2p orbitals. In previous experiments, the full S $L_{2,3}$MM Auger electron spectrum was measured,[24] and thus the analysis of the spectrum and the comparison with the theoretical models had to rely on the hypothesis that the spectrum consists of two groups of peaks shifted by the spin−orbit separation and weighted by a factor of 2:1. The same approach has been followed in the theoretical paper by Minelli et al.[29] for the simulation of the experimental spectrum. Here where the "pure" S L_3MM has been measured via a coincidence experiment, a more direct and detailed comparison between experiments and theory can be performed.

The L_3MM Auger spectrum can be divided into three main regions. The first one extends from 141.5 to 136.5 eV Auger energy, that is, from 29.15 to 34.15 eV DIE. The three main features of this region correspond to the removal of two electrons from the 3π outermost occupied orbital. This results in the first three states of the OCS^{2+} dication with $^3\Sigma^-$, $^1\Delta$, and $^1\Sigma^+$ configurations. The relative $^1\Delta-^3\Sigma^-$ and $^1\Sigma^+-^3\Sigma^-$ energy differences are 0.95 ± 0.1 and 1.78 ± 0.1 eV, which is in good agreement with the values extracted from the full L_{23}MM experimental spectrum by Carroll et al.[24] and the theoretical calculations of the DIE by Millie et al.[30] In the second region (136.5−131.5 eV Auger energy and 34.15−39.15 eV DIE), Auger states built on the $9\sigma 3\pi$, $8\sigma 3\pi$, and $2\pi 3\pi$ configurations are expected to occur. The first two configurations yield $^3\Pi$ and $^1\Pi$ terms, whereas the last configuration gives six terms ($^{3,1}\Sigma^-$, $^{3,1}\Delta$, and $^{3,1}\Sigma^+$). In our spectrum, four clear features can be observed. They have been assigned to the $^3\Pi$ and $^1\Pi$ terms of the $9\sigma 3\pi$, $8\sigma 3\pi$ configurations. The relative distances (5.11, 6.025, 6.72, 7.28 eV) with respect to the $^3\Sigma^-$ ground state of OCS^{2+} are consistent with the ones obtained by Carroll et al.[24] To achieve an acceptable fit, we have considered a few other minor peaks, with an intensity that amounts to about 12% of the full intensity in this region. They likely can be assigned to dication states with $2\pi 3\pi$ configurations. The assignment proposed for this region is supported by the population analysis of the 2hole pole strengths done by Minelli et al.[29] In the region between 131.5 and 126 eV Auger energy (39.15−44.65 eV DIE), a broad structure extending over about 3 eV and then a double-peaked feature are observed. The main contribution to the broad structure is due to states with configuration $2\pi 9\sigma$,[24,29,30] and their low intensity is due to the small 2π density on sulfur.[24,29] The other feature in this region is easily decomposed into two peaks that can be assigned to $9\sigma^2$ and $9\sigma 8\sigma$ configurations (peaks at 13.37 and 12.42 eV from the $^3\Sigma^-$ ground state of OCS^{2+}, respectively).

In Figure 3, the experimental L_3MM Auger spectrum is compared with that calculated by Minelli et al.[29] The two-particle Green's function algebraic diagrammatic construction (ADC) method[31] used by these authors is an efficient method to compute directly double ionization spectra of polyatomic molecules. Its application together with a two-hole atomic population analysis and the consideration of the nuclear dynamics of the decaying states provides quantitative information on the hole localization in the final states, an adequate estimate of the Auger intensity distribution, and a simulation of the nuclear dynamics, which results in a shift and broadening of the bands.

Minelli et al.[29] represented each transition of the theoretical spectra by a Lorentzian function whose centroid and width are obtained from the vibrational analysis and reported in table III of ref 29. Moreover, to account for the experimental resolution, they added the experimental uncertainty to the calculated width. For the sake of consistency with ref 29, in the comparison of Figure 3, the value of 0.6 eV, which represents the experimental uncertainty for the Auger electrons, has been added to the calculated width. The relative intensities of the different states have been estimated using the S^{2-} 2hole population analysis reported in table I of ref 29. The procedure is not expected to be very accurate for a specific state but gives a readily obtainable and reliable picture of the distribution of the relative intensities in the spectrum.

The theory calculates the $^3\Sigma^-$ ground state of OCS^{2+} to be 29.43 eV, that is, about 0.9 eV lower than the measured value. Therefore, we have shifted all theoretical predictions by this amount.

The comparison shows that the theory satisfactorily reproduces all main features of the spectrum. However, a displacement of the position of the features as the DIE increases is observed, and the features in the theoretical spectrum appear to be broader than those in the experimental spectrum. The inaccuracy in the peak positions of the theoretical spectrum are expected to be 0.1 to 0.2 eV up to DIE = 40 eV and then to increase to about 0.5 eV.[29] We found that the difference between theory and experiment amounts to 0.35 eV already in the region of DIE = 35 eV and then increases up to 0.7 eV at DIE = 44 eV. A good agreement between theory and experiment can be achieved by contracting the theoretical scale by a factor 0.95. (See the inset in Figure 3.) The broadening of the theoretical line shape might be attributed to an overestimation of the nuclear dynamics effects. As far as the relative intensities are concerned, the satisfactory agreement obtained up to 38 eV degrades for

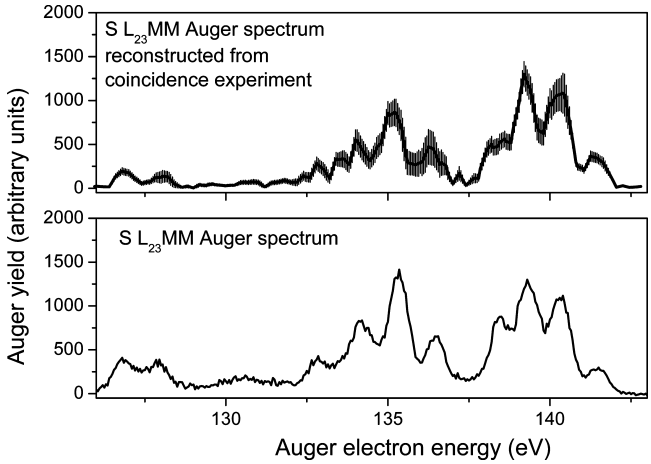

Figure 4. Comparison between the S LMM Auger electron (bottom) and reconstructed photoelectron−Auger electron coincidence (top) spectrum. The uncertainty in the reconstructed spectrum is obtained via error propagation from the uncertainty of the measured L_3MM coincidence spectrum.

higher DIE. Significantly larger intensity is predicted for the region $9\sigma^{-2}$ and $9\sigma^{-1}8\sigma^{-1}$ states at about 45 eV. The number of active transitions increases substantially in the region above 40 eV,[29] and, as a consequence, the enhanced correlation effects are more difficult to reproduce.

Finally, the measured coincidence L_3MM spectrum can be used to reconstruct the full S LMM Auger spectrum. This can be done under the assumption that the two spin−orbit components produce Auger spectra separated by the spin−orbit separation and weighted by their relative photoionization cross section. Therefore, we have interpolated the measured L_3MM spectrum and then reconstructed the full LMM spectrum using these assumptions. The reconstructed LMM spectrum is shown in Figure 4, where it is compared with the noncoincidence spectrum. The two spectra are in agreement within the uncertainties of the coincidence experiment in the regions 141.5−136.5 and 129−126 eV. The feature at about 135.3 eV is significantly more intense in the noncoincidence spectrum than in the coincidence one. In the region 135−132 eV, the features in the noncoincidence spectrum are broader than those in the coincidence spectrum, which is likely because of some partially overlapping structures that are not present in the coincidence spectrum. At about 130 eV, the noncoincidence spectrum displays a broad feature that is barely visible in the coincidence measurements. These observations lead to the conclusion that there are contributions to the noncoincidence spectrum that are not generated by the decay of the 2p holes. Two shakeup satellites at 9.5 and 15 eV above the 2p threshold have been reported in the literature.[32,15] Their intensity has been observed to increase moving toward their respective thresholds. Moreover, a recent work[33] on SF_6 has shown that approaching the S 2p threshold, several conjugate shakeup satellites can also be excited. The Auger decay of these satellites to excited states of the dication may explain the extra intensity observed in the noncoincidence spectrum.

3.2. Auger Electron Angular Distributions. The angular distribution of the Auger electrons has been measured in a noncoincidence experiment at about 200 eV photon energy (Figure 5) and via photoelectron−Auger electron coincidence experiments at about 178 and 200 eV photon energies (Figure 6). In the latter experiments, only the angular distributions of the Auger electrons leading to the $OCS2^+$ $^1\Sigma^+$ and $^1\Delta$ final states have been measured.

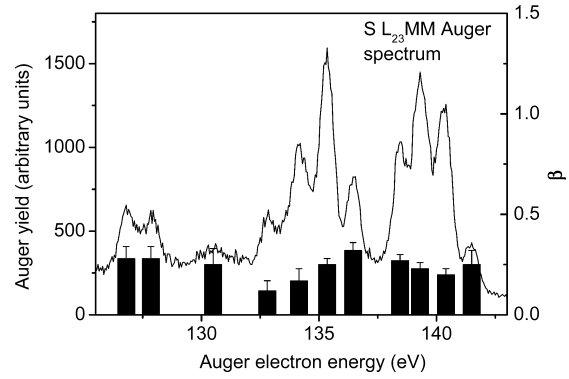

Figure 5. Asymmetry parameters measured in a noncoincidence experiment for several features of the S $L_{2,3}MM$ Auger electron spectrum.

The asymmetry parameter β for the different features in the noncoincidence spectrum has been determined using the spectra measured simultaneously at 0 and 90° with respect to the direction of the axis of polarization of the incident radiation. All features in the spectrum (Figure 5) display a positive, nonvanishing β value with an average value of about 0.21 ± 0.06.

In the case of the photoelectron−Auger electron coincidence measurements, the experiments have been performed at two different photon energies (178 and 200 eV) in the case of the $^1\Delta$ state and only at 178 eV for the $^1\Sigma^+$ state. The energy of 178 eV corresponds to the broad shape resonance in the continuum observed in the NEXAFS spectrum.[20] In all cases, the photoelectron has been detected along the direction of polarization of the incident radiation. The coincidence angular distributions display a shape different from the noncoincidence distribution, measured simultaneously. Moreover, the shape of the coincidence angular distribution shows a clear dependence on the incident energy and on the selected final dication state. In the case of the measurements in the shape resonance, the Auger electrons are preferentially emitted along the direction of polarization with a contribution in the perpendicular direction, which varies from the $^1\Delta$ and $^1\Sigma^+$ states (Figure 6a,b). A fit with an expansion of Legendre polynomials ($Y_{\text{fit}} = \sum_{k=0}^{2l_{\max}} a_k P_k(\cos\theta)$), where θ is the relative angle between the directions of the Auger electron and the photoelectron, shows that the coincidence angular distributions are well described by the even terms of the expansion with $\mathbf{l}_{\max} = 2$. By increasing the energy, a strong asymmetry in the coincidence angular distribution is observed (Figure 6c), and the Auger electrons appear to be preferentially emitted opposite to the direction of the photoelectron. In this case, a truncation at $\mathbf{l}_{\max} = 2$ and the inclusion of odd terms in the polynomial expansion result in a satisfactory representation of the data. The maximum of the expansion reflects the dipole character of the primary photoionization process, whereas the need for the odd terms results from the reduction of the symmetry observed in Figure 6c with respect to Figure 6b. Indeed, in Figure 6b, the coincidence distribution displays a symmetry with respect to both the polarization axis and the plane perpendicular to this axis, whereas in Figure 5c, only the symmetry about the direction of the polarization of the incident radiation and of the photoelectron is observed. A similar observation was reported for the C1s photoionization in CO studied via a photoelectron−Auger electron coincidence experiment.[14] In the case of the CO^{2+} X state, a noticeable change of the shape of the angular distribution was observed moving off the σ^* shape resonance. This observation was rationalized

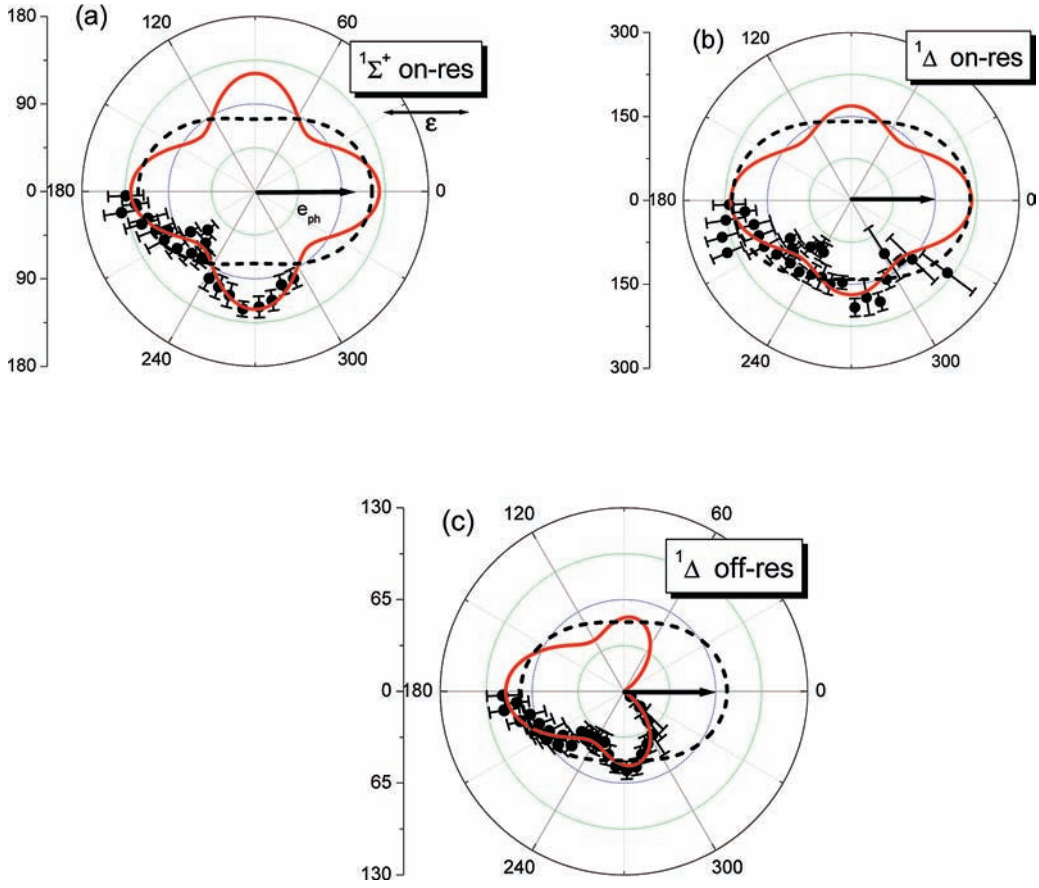

Figure 6. S $2p_{3/2}$ photoelectron−Auger electron coincidence angular distributions for the OCS^{2+} $^1\Sigma^+$(panel a) and $^1\Delta$ (panel b and c) states. The measurements labeled "on-resonance" (panels a and b) have been done at a photon energy of 178 eV, whereas the one labeled "off-resonance" (panel c) has been done at 200 eV photon energy. In all of the measurements, the photoelectron has been detected (see black arrows in all panels) in the direction of the polarization axis of the incident radiation. The full (red) curve is a fit to the experimental data with an expansion of Legendre polynomials (see the text), whereas the dashed (black) curve is the noncoincidence angular distribution of the Auger electrons measured simultaneously to the photoelectron−Auger electron coincidence angular distributions.

considering that in the photoionization of the C1s orbital in the region of the σ^* shape resonance the photoelectrons are emitted preferentially in the direction of the O atoms. Therefore, the molecular axis of CO^+ appears to be partially oriented. Calculations[14] then showed that this also leads to a pronounced asymmetry in the emission of the Auger electrons in fixed-in-space CO molecules, but a trace of the effect also remains in the photoelectron−Auger electron angular distribution[14] of randomly oriented molecules. The recent study of the photoionization of the S 2p state in fixed-in-space OCS molecules by Golovin et al.[16] has proved that the angular distribution of the S 2p photoelectrons is characterized by a preferential emission in a solid cone directed from the molecular center to the S atom when the incident radiation is linearly polarized along the molecular axis. This asymmetry has been observed to increase when the photon energy increases from 174 to 198 eV. Therefore, we may infer that by analogy to the CO case this may lead to a preferential orientation of the molecular axis that then results in an asymmetric emission of the Auger electrons, as observed in the photoelectron−Auger electron angular distribution.

Figure 6b,c share the same dication final state and the same direction of the photoelectron. The difference remains only in the energy of photon. The variation of the shape of the angular distribution with the photon energy gives hints that despite the quite long lifetime of the S 2p hole [$\Gamma = 65$ meV[21]] the primary photoionization process and the cation relaxation via Auger emission are not completely uncorrelated, at least in the energy region investigated in this work. Models based on the two-step approximation, such as the one proposed by Semenov et al.,[14] treat the formation of the core hole and the following nonradiative decay separately. The links between the two are given by parameters that contain the dipole matrix elements for the photoionization. These parameters determine the overall intensity of the Auger angular distribution as a function of incident energy but not its shape. Therefore, the present observations as well as the ones of the CO C Auger angular distribution in the molecular frame[34] call for models that go beyond the two-step approximation.

The photoelectron−Auger electron coincidence experiments have been proposed[35] and proved, in the case of atoms,[5,36] to be "complete experiments", where the transition amplitudes and relative phases of either the photoionization or the Auger decay can be obtained experimentally. In linear molecules, the complete information on the photoionization process can be extracted by the measurement of the photoelectron angular distribution of "fixed-in-space" molecules. Semenov et al.[14] theoretically showed that photoelectron−Auger electron coincidence angular distribution can provide valuable information on the decay process. Unfortunately, the investigation of the CO C1s photoionization and decay via this technique[14] showed that independent of the photon energy used and of the final CO^{2+} state, the measured angular distributions were almost isotropic and not sensitive enough to the details of the Auger electron wave function. The observed variation in shape of the measured coincidence angular distributions for the case of S 2p gives hope

that a proper theoretical model may lead to the extraction of the basic information on the Auger decay from these coincidence experiments.

4. Conclusions

The S L_3MM Auger spectrum has been measured via a photoelectron−Auger electron coincidence technique. This has allowed a precise assignment of the final dication states and an accurate comparison with the calculated spectra in the framework of the two-particle Green's function ADC method.[29] It is shown that the theory tends to overestimate the energies of the states as the DIE increases and also tends to predict too broad peaks. As far as the relative intensity is concerned, the approximation to use the 2 h population on the S atom appeared to work satisfactorily up to a region where correlation effects play a major role.

The measurements of the photoelectron−Auger electron coincidence angular distributions, in contrast with previous experiments on the CO C1s case,[14] show sensitivity to both incident energy and final dication states. The observed correlation between the photoionization and Auger process, which questions the widely used two-step approximation, has been the subject of a controversy because of some measurements of the Auger angular distribution in fixed-in-space CO molecules.[35,37,38] The present results add further evidence that in the investigated energy region the formation and decay of the inner hole cannot be treated as uncorrelated processes. Moreover, they indicate that photoelectron−Auger electron coincidence experiments in the case of the ionization of a p orbital and in a suitable experimental geometry should be reconsidered for the extraction of the matrix elements of the molecular Auger process.

Acknowledgment. This work was partially supported by the MIUR-FIRB Program "Probing the microscopic dynamics of chemical reactivity" and by the MIUR-FIRB "SPARX".

References and Notes

(1) Thompson, M.; Baker, M. D.; Christie, A.; Tyson, J. F. *Auger Electron Spectroscopy*; John Wiley & Sons: New York, 1985.
(2) Tarantelli, F.; Sgamellotti, A.; Cederbaum, L. S. *J. Electron Spectrosc. Relat. Phenom.* **1994**, *68*, 297.
(3) Haak, H. W.; Sawatzky, G. A.; Thomas, T. D. *Phys. Rev. Lett.* **1978**, *41*, 1825.
(4) von Raven, E.; Meyer, M.; Pahler, M.; Sonntag, B. *J. Electron Spectrosc. Relat. Phenom.* **1990**, *52*, 677.
(5) Kämmerling, B.; Schmidt, V. *Phys. Rev. Lett.* **1991**, *67*, 1848; **1992**, *69*, 1145.
(6) Bartynski, R. A.; Yang, S.; Hubert, S. C.; Kao, C.-C.; Weinert, M.; Zehner, D. *Phys. Rev. Lett.* **1992**, *68*, 2247.
(7) Viefhaus, J.; Snell, G.; Hentges, R.; Wiedenhöft, M.; Heiser, F.; Geβner, O.; Becker, U. *Phys. Rev. Lett.* **1998**, *80*, 1618.
(8) Prince, K. C.; Blyth, R. R.; Delaunay, R.; Zitnik, M.; Krempasky, J.; Slezak, J.; Camilloni, R.; Avaldi, L.; Coreno, M.; Stefani, G.; Furlani, C.; de Simone, M.; Stranges, S. *J. Synchrotron Radiat.* **1998**, *5*, 565.
(9) Bolognesi, P.; Coreno, M.; Avaldi, L.; Storchi, L.; Tarantelli, F. *J. Chem. Phys.* **2006**, *125*, 54306.
(10) Bolognesi, P.; Püttner, R.; Avaldi, L. *Chem. Phys. Lett.* **2008**, *464*, 21.
(11) Dill, D.; Swanson, J. R.; Wallace, S.; Dehmer, J. L. *Phys. Rev. Lett.* **1980**, *45*, 1393.
(12) Becker, U.; Hölzel, R.; Kerkhoff, H. G.; Langer, B.; Szostak, D.; Wehlitz, R. *Phys. Rev. Lett.* **1986**, *56*, 1455.
(13) Kivimäki, A.; Neeb, M.; Kempgens, B.; Köppe, H. M.; Bradshaw, A. M. *Phys. Rev.* **1996**, *A 54*, 2137.
(14) Semenov, S. K.; Kuznestov, V. V.; Cherepkov, N. A.; Bolognesi, P.; Feyer, V.; Lahmam-Bennani, A.; Staicu Casagrande, M. E.; Avaldi, L. *Phys. Rev.* **2007**, *A75*, 32707.
(15) Truesdale, C. M.; Lindle, D. W.; Kobin, P. H.; Becker, U. E.; Kerkhoff, H. G.; Heimann, P. A.; Ferrett, T. A.; Shirley, D. A. *J. Chem. Phys.* **1984**, *80*, 2319.
(16) Golovin, A. V.; Adachi, J.; Motoki, S.; Takahashi, M.; Yagishita, A. *J. Phys. B: At. Mol. Opt. Phys.* **2005**, *38*, L63.
(17) Golovin, A. V.; Adachi, J.; Motoki, S.; Takahashi, M.; Yagishita, A. *J. Phys. B: At. Mol. Opt. Phys.* **2005**, *38*, 3755.
(18) Blyth, R. R.; Delaunay, R.; Zitnik, M.; Krempasky, J.; Krempaska, R.; Slezak, J.; Prince, K. C.; Richter, R.; Vondracek, M.; Camilloni, R.; Avaldi, L.; Coreno, M.; Stefani, G.; Furlani, C.; de Simone, M.; Stranges, S.; Adam, M. Y. *J. Electron Spectrosc. Relat. Phenom.* **1999**, *959*, 101–103.
(19) Melpignano, P.; Di Fonzo, S.; Bianco, A.; Jark, W. *Rev. Sci. Instrum.* **1995**, *66*, 2125.
(20) Magnuson, M.; Guo, J.; Säthe, C.; Rubensson, J.-E.; Nordgren, J.; Glans, P.; Yang, L.; Salek, P.; Ågren, H. *Phys. Rev. A* **1999**, *59*, 4281.
(21) Kukk, E.; Bozek, J. D.; Sheenhy, J. A.; Langhoff, P. W.; Berrah, N. *J. Phys. B: At. Mol. Opt. Phys.* **2000**, *33*, L51.
(22) van der Straten, P.; Mongerstern, R.; Niehaus, A. *Z. Phys.* **1988**, *D8*, 35.
(23) Sourworth, S. H.; Kobrin, P. H.; Truesdale, C. M.; Lindle, D.; Owaki, S.; Shirley, D. A. *Phys. Rev.* **1981**, *A24*, 2257.
(24) Carroll, T. X.; Ji, De; Thomas, T. D. *J. Electron Spectrosc. Relat. Phenom.* **1990**, *51*, 471.
(25) Cooks, R. G.; Terwillinger, D. T.; Beynon, J. H. *J. Chem. Phys.* **1981**, *61*, 171.
(26) Griffiths, W.G.; Harris, F. M. *Int. J. Mass Spectrom. Ion Processes* **1989**, *87*, 349. Langford, M. L.; Harris, F. M.; Reid, C. J.; Ballantine, J. A.; Parry, D. E. *Chem. Phys.* **1991**, *149*, 445.
(27) Jonathan, P.; Hamdam, M.; Brenton, G. *Chem. Phys.* **1988**, *119*, 159.
(28) Hall, R. I.; Avaldi, L.; Dawber, G.; McConkey, A. G.; MacDonald, M. A.; King, G. C. *Chem. Phys.* **1994**, *187*, 125.
(29) Minelli, D.; Tarantelli, F.; Sgamellotti, A.; Cederbaum, L. S. *J. Chem. Phys.* **1997**, *107*, 6070.
(30) Millie, P.; Nenner, I.; Archirel, P.; Lablanquie, P.; Fournier, P.; Eland, J. H. D. *J. Chem. Phys.* **1986**, *84*, 1259.
(31) Tarantelli, F.; Sgamellotti, A.; Cederbaum, L. S. *J. Chem. Phys.* **1991**, *94*, 523.
(32) Allan, C. J.; Gelius, U.; Allison, D. A.; Johansson, G.; Siegbgahn, H.; Siegbahn, K. *J. Electron Spectrosc. Relat. Phenom.* **1973**, *1*, 131.
(33) Decleva, P.; Fronzoni, G.; Kivimäki, A.; Álvarez Ruiz, J.; Svensson, S. *J. Phys. B: At. Mol. Opt. Phys.* **2009**, *42*, 55102.
(34) Guillemin, R.; Shigemasa, E.; Le Guen, K.; Ceolin, D.; Miron, C.; Leclercq, N.; Morin, P.; Simon, M. *Phys. Rev. Lett.* **2001**, *87*, 203001.
(35) Kabachnik, N. M. *J. Phys. B: At. Mol. Opt. Phys.* **1992**, *25*, L389.
(36) Bolognesi, P.; De Fanis, A.; Coreno, M.; Avaldi, L. *Phys. Rev. A* **2004**, *A70*, 022701; **2005**, *A72*, 069903.
(37) Weber, Th.; Weckenbrock, M.; Balser, M.; Schmidt, L.; Jagutzki, O.; Arnold, W.; Hohn, O.; Schöffler, M.; Arenholz, E.; Young, T.; Osipov, T.; Foucar, L.; De Fanis, A.; Dıez Muiño, R.; Schmidt-Böcking, H.; Cocke, C. L.; Prior, M. H.; Dörner1, R. *Phys. Rev. Lett.* **2003**, *90*, 153003.
(38) Prümper, G.; Fukuzawa, H.; Rolles, D.; Sakai, K.; Prince, K. C.; Harries, J. R.; Tamenori, Y.; Berrah, N.; Ueda, K. *Phys. Rev. Lett.* **2008**, *101*, 233202.

JP9053007